CHAPTER 7 METHODS TO PREDICT MINOR LOSS DUE TO MEANDER BENDS

In order to better estimate cross-sectional average total energy loss ($\bar{h}_t$) given HEC-RAS output, a method needed to be developed to predict cross-sectional average minor loss due to a meander bend ($\bar{h}_{BEND}$). Predictor methods aid understanding of the relationship between geometry of a meander bend and discharge through a meander bend through an equation. During this analysis, a predictor method was developed to calculate cross-sectional average minor loss due to a meander bend. This method established a relationship between minor loss due to a meander bend and a pi term. The pi term was a dimensionless ratio relating external, material, and channel properties during the base-line analysis. Detailed methodology is discussed in the succeeding sections.

7.1 DEVELOPMENT OF THE METHOD

A method was established to calculate cross-sectional average minor loss due to a meander bend in order to estimate cross-sectional average total energy loss and, therefore, average total energy loss through a meander bend ($\bar{h}_T$) given HEC-RAS output. This method used a dimensionless pi term to establish a relationship with the ratio, $\bar{h}_{BEND}/\bar{h}_{Sf}$. A dimensionless relationship allowed the method developed with the

physical model to be used outside the laboratory and in natural river systems. Steps used to formulate a significant pi term are discussed in Section 7.1.1.

7.1.1 Development of a Pi Term

To develop a pi term demonstrating a significant relationship to the observed $\bar{h}_{BEND}/\bar{h}_{Sf}$, various pi terms were developed as a function of material, channel, and external properties. Variables that define material, channel, and external properties are outlined in Table 7.1.

Table 7.1. Variables Describing Dimensionless Pi Terms

Material Properties		
Symbol	Definition	Dimensions
υ	Kinematic Viscosity of Water	L^2/T
ρ	Density of Water	M/L^3
μ	Dynamic Viscosity of Water	$M\text{-}T/L^2$

Channel Properties		
Symbol	Definition	Dimensions
S_o	Bed Slope	
TW	Top Width	L
r_c	Radius of Curvature	L
L_b	Length of Channel Bend Along Centerline	L
y	Flow Depth	L
BW	Base Width	L
A	Cross-sectional Area	L^2
n	Manning's Roughness	

External Properties		
Symbol	Definition	Dimensions
Q	Discharge	L^3/T
g	Acceleration of Gravity	L/T^2

In this analysis, twenty-three pi terms were developed to determine a pi term that displayed a significant relationship with the observed $\bar{h}_{BEND}/\bar{h}_{Sf}$. Table 7.2 lists the twenty-three pi terms developed for this analysis.

Table 7.2. Relationships Describing Each Pi Term

Pi Term	Pi Term Relationship	Pi Term	Pi Term Relationship
π_1	$(r_c/TW)^2 / (Fr * 10)$	π_{13}	$(g * TW^2 * BW^2 * r_c / Q * \upsilon) * (S_o / 10^6)$
π_2	Fr	π_{14}	$(Q / (\upsilon * TW * BW)) * S_o$
π_3	$(TW / r_c) * S_o$	π_{15}	$(Q / (\upsilon * (TW - y_{PG}) * BW)) * S_o$
π_4	TW / y_{PG}	π_{16}	$(\upsilon * y_{PG} * r_c) / Q$
π_5	r_c / TW	π_{17}	π_6^{-1}
π_6	$(r_c / BW) * (y_{PG} / TW) * 100$	π_{18}	π_7^{-2}
π_7	$[(r_c / BW) * (y_{PG} / TW) * 100] * Fr$	π_{19}	π_9^{-1}
π_8	$(r_c / BW) * (S_o / Fr)$	π_{20}	$Q / (g^{1/2} * r_c^{1.5} * y_{PG})$
π_9	$(TW / BW) * S_o * 1000$	π_{21}	$(g^{1/2} * r_c^{1.5}) / v_{AVG}$
π_{10}	$(r_c / L_b) * (TW / BW)$	π_{22}	$\pi_2 * \pi_{20}$
π_{11}	r_c / y_{PG}	π_{23}	$\pi_{22} * (L_b / y_{PG})$
π_{12}	$(Q * \upsilon) / (g * TW^2 * BW^2 * r_c)$		

In order to compare the twenty-three pi terms outlined in Table 7.2, the subsequent methodology is followed:

1. Plot observed $\bar{h}_{BEND}/\bar{h}_{Sf}$ vs. π in Microsoft® Excel;
2. Determine a trend line using graphical functions in Microsoft® Excel that interpolates a significant relationship between observed $\bar{h}_{BEND}/\bar{h}_{Sf}$ and π;
3. Use equation defining interpolated trend line to calculate predicted $\bar{h}_{BEND}/\bar{h}_{Sf}$;

4. Calculate percent error and absolute percent error between predicted $\overline{h}_{BEND}/\overline{h}_{Sf}$ and observed $\overline{h}_{BEND}/\overline{h}_{Sf}$;
5. Plot observed $\overline{h}_{BEND}/\overline{h}_{Sf}$ vs. predicted $\overline{h}_{BEND}/\overline{h}_{Sf}$ to observe linear relationship;
6. Rank pi terms according to calculated percent error and absolute percent error; and
7. Select most significant π.

Appendix D illustrates Step 1 through Step 5 for π_5. From the list of 23 pi terms, π_5 demonstrated the most significant relationship to the observed $\overline{h}_{BEND}/\overline{h}_{Sf}$. Equation 7.1 notes the dimensionless relationship established in π_5:

$$\pi_5 = \frac{r_c}{\overline{TW}} \qquad \textbf{Equation 7.1}$$

where:

π_5 = dimensionless term;

r_c = radius of curvature (ft); and

$\overline{TW}$ = cross-sectional average top width (ft).

Once π_5 was selected as the most significant pi term, the graphical relationship was used to calculate the predicted cross-sectional average minor loss due to a meander bend. The graphical relationship established for π_5 is discussed in the succeeding section.

7.1.2 Graphical Relationship

A graphical relationship was established which showed a significant correlation between π_5 and observed $\overline{h}_{BEND}/\overline{h}_{Sf}$. This relationship is illustrated in Figure 7.1. As

Figure 7.1 illustrates, the graphical relationship between π_5 and observed $\bar{h}_{BEND}/\bar{h}_{Sf}$ was formulated by interpolating an exponential trend line in Microsoft® Excel. Equation 7.2 presents the numerical relationship of the exponential trend line:

$$\frac{\bar{h}_{BEND}}{\bar{h}_{Sf}} = 4.0e^{-0.45\pi_5} \qquad \textbf{Equation 7.2}$$

where:

$\bar{h}_{BEND}$ = cross-sectional average minor loss due to meander bend (ft);

$\bar{h}_{Sf}$ = cross-sectional average, average friction loss (ft); and

π_5 = dimensionless term.

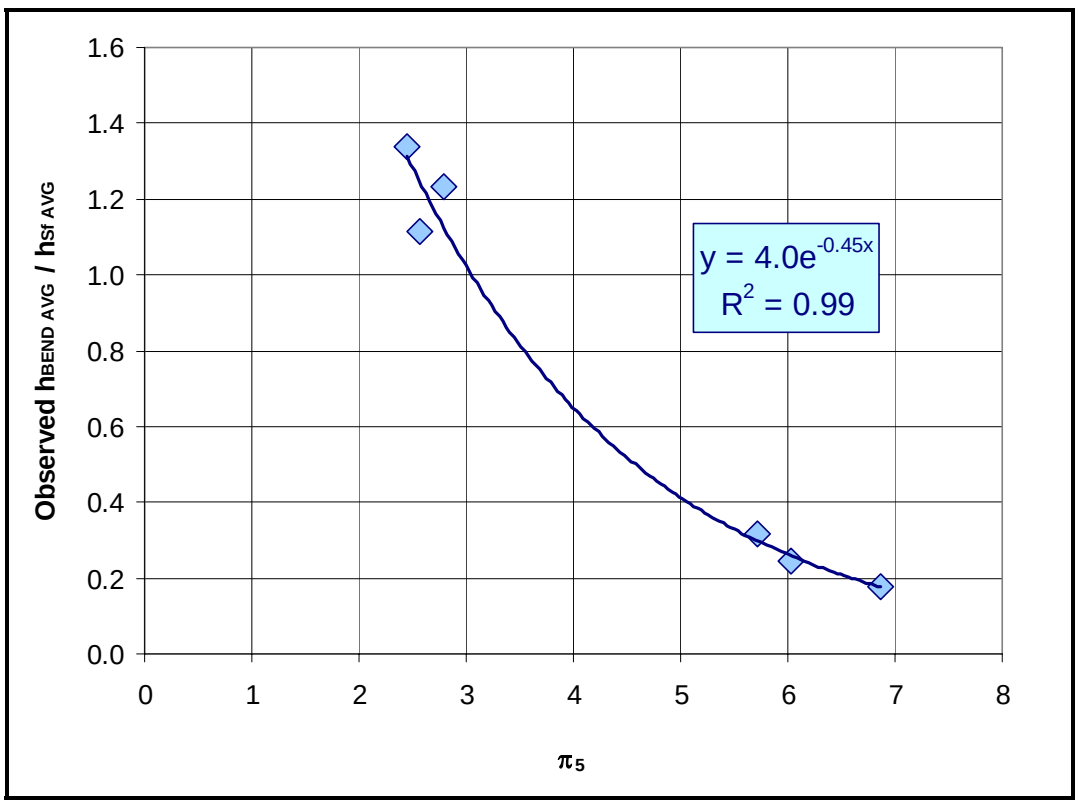

Figure 7.1. Graphical Relationship Between π_5 and Observed $\bar{h}_{BEND}/\bar{h}_{Sf}$

The relationship developed in Equation 7.2 was used to calculate cross-sectional average minor loss due to a meander bend with Equation 7.3:

$$\bar{h}_{BEND} = \bar{h}_{Sf}\left(\frac{\bar{h}_{BEND}}{\bar{h}_{Sf}}\right) \qquad \textbf{Equation 7.3}$$

where:

$\bar{h}_{BEND}$ = cross-sectional average minor loss due to meander bend (ft); and

$\bar{h}_{Sf}$ = cross-sectional average, average friction loss (ft).

Once Equation 7.1 through Equation 7.3 were established, a methodology was developed in order to outline the steps required to predict cross-sectional average minor loss due to a meander bend. This method was referred to as the π_5 method and is outlined in Section 7.1.3.

7.1.3 π_5 Method Used to Calculate Predicted $\bar{h}_{BEND}$

A method was needed to predict cross-sectional average minor loss due to a meander bend based on Equation 7.1 through Equation 7.3. The method is outlined as follows:

1. Define project area:
    a. location of study reach;
    b. type of river; and
    c. length of river.
2. Collect appropriate data during site assessment:
    a. Cross-sectional survey;
    b. Thalweg survey along meander bend;

c. Roughness coefficients:

   i. channel;

   ii. left overbank; and

   iii. right overbank.

d. Note channel contractions or expansions along meander bend.

e. Perform the following tasks **IF** time and equipment permits:

   i. record cross-sectional average discharge at each cross section;

   ii. flow-depth measurements along thalweg; and

   iii. flow-depth measurements downstream of meander bend.

3. If time and equipment **DID NOT** permit collecting data in Step 2, Part e:

   a. collect stage vs. discharge record for study reach.

4. Build HEC-RAS model with data collected during site assessment.

5. Run HEC-RAS model.

6. Use data collected during Step 2, Part e OR Step 3 to check that HEC-RAS accurately predicts flow depths through study reach.

7. Calculate $\overline{TW}$:

   a. copy top width estimates from HEC-RAS output table into Microsoft® Excel; and

   b. calculate $\overline{TW}$ through meander bend.

8. Estimate r_c with aerial photographs.

9. Calculate π_5.

10. Estimate $\overline{h}_{BEND}/\overline{h}_{Sf}$ with relationship presented in Equation 7.2.

11. Calculate $\overline{h}_{BEND}$:

a. copy h_{Sf} estimates from HEC-RAS output table into Microsoft® Excel;

b. calculate $\overline{h}_{Sf}$ through meander bend; and

c. calculate $\overline{h}_{BEND}$ with Equation 7.3.

Based on this methodology, results for predicted cross-sectional average minor loss due to a meander bend in the Type I and Type III bends are shown in Table 7.3 at discharges of 8 cfs, 12 cfs, and 16 cfs. Results of cross-sectional average minor loss due to a meander bend are used in Section 7.2 to determine cross-sectional average total energy loss.

Table 7.3. $\overline{h}_{BEND}$ Results Using π_5 Method

Bend	Q (cfs)	$\overline{h}_{BEND}$ (ft)
Type I (U/S) Bend	8	0.0028
	12	0.0025
	16	0.0029
Type III (D/S) Bend	8	0.0012
	12	0.0013
	16	0.0017

Steps used in the π_5 method determined cross-sectional average minor loss due to a meander bend. In order to calculate average minor loss due to a meander bend through a meander bend ($\overline{h}_{BEND-TOTAL}$), use Equation 6.2.

7.2 TOTAL ENERGY LOSS CALCULATION

Ultimately, the goal of this analysis is to accurately calculate the average total energy loss through a meander bend using HEC-RAS output. The π_5 method stated in Section 7.1.3 determined the predicted cross-sectional average minor loss due to a meander bend and these results are used in the calculation for cross-sectional average

total energy loss and average total energy loss through the meander bend ($\bar{h}_T$). Cross-sectional average total energy loss is calculated with Equation 7.4:

$$\bar{h}_t = \bar{h}_{BEND} + \bar{h}_{Sf} \qquad \textbf{Equation 7.4}$$

where:

$\bar{h}_{BEND}$ = cross-sectional average minor loss due to meander bend (ft);

$\bar{h}_{Sf}$ = cross-sectional average, average friction loss (ft); and

$\bar{h}_t$ = cross-sectional average total energy loss (ft).

Average total energy loss through a meander bend is calculated with Equation 7.5:

$$\bar{h}_T = \left(XS_{TOTAL} - 1\right)\bar{h}_t \qquad \textbf{Equation 7.5}$$

where:

$\bar{h}_t$ = cross-sectional average total energy loss (ft);

$\bar{h}_T$ = average total energy loss through meander bend (ft); and

XS_{TOTAL} = number of cross sections used in analysis.

Results for average total energy loss through a meander bend using the π_5 method were compared to average total energy loss through meander bend estimates using unmodified HEC-RAS output and physical model measurements. These results are shown for discharges of 8 cfs, 12 cfs, and 16 cfs in Table 7.4, Table 7.5, and Table 7.6, respectively. As Table 7.4 through Table 7.6 illustrate, the average total energy loss through a meander bend calculated with the π_5 method is more accurate than the average total energy loss through meander bend results estimated with unmodified HEC-RAS output in both the Type I and Type III bends.

Table 7.4. $\bar{h}_T$ Results at 8 cfs

Bend	$\bar{h}_T$ (ft)		
	Physical Model Measurements	Unmodified HEC-RAS Output	π_5 Method
Type I (U/S) Bend	0.0216	0.0104	0.0211
Type III (D/S) Bend	0.0386	0.0364	0.0395
Absolute Difference From Physical Model $\bar{h}_T$			
	Type I (U/S) Bend	0.0112	0.0005
	Type III (D/S) Bend	0.0022	0.0010

Table 7.5. $\bar{h}_T$ Results at 12 cfs

Bend	$\bar{h}_T$ (ft)		
	Physical Model Measurements	Unmodified HEC-RAS Output	π_5 Method
Type I (U/S) Bend	0.0162	0.0085	0.0180
Type III (D/S) Bend	0.0291	0.0272	0.0307
Absolute Difference From Physical Model $\bar{h}_T$			
	Type I (U/S) Bend	0.0078	0.0018
	Type III (D/S) Bend	0.0019	0.0017

Table 7.6. $\bar{h}_T$ Results at 16 cfs

Bend	$\bar{h}_T$ (ft)		
	Physical Model Measurements	Unmodified HEC-RAS Output	π_5 Method
Type I (U/S) Bend	0.0200	0.0092	0.0202
Type III (D/S) Bend	0.0359	0.0315	0.0369
Absolute Difference From Physical Model $\bar{h}_T$			
	Type I (U/S) Bend	0.0108	0.0002
	Type III (D/S) Bend	0.0044	0.0010

In the Type I bend at a discharge of 8 cfs, physical model measurements suggest that the average total energy loss through a meander bend in the Type I bend is 0.0216 ft. The π_5 method calculates an average total energy loss of 0.0211 ft, which is 2% different from the physical model measurements. At the same discharge in the Type I bend, the

average total energy loss through a meander bend is equal to 0.0104 ft for the unmodified HEC-RAS output, which is a difference of 52% from the physical model data set. This pattern is followed at discharges of 12 cfs and 16 cfs.

In the Type III bend, the π_5 method continues to estimate average total energy loss through a meander bend more accurately than the unmodified HEC-RAS data set. In the Type III bend at a discharge of 16 cfs, physical model measurements suggest that the average total energy loss through a meander bend in the Type III bend is 0.0359 ft. The π_5 method calculates an average total energy loss of 0.0369 ft, which is 3% different from the physical model measurements. At the same discharge in the Type III bend, the average total energy loss through a meander bend is 0.0315 ft for the unmodified HEC-RAS output, which is a difference of 12%. This pattern is followed at discharges of 8 cfs and 12 cfs.

A possible reason that HEC-RAS estimates average total energy loss through a meander bend more accurately in the Type III bend than in the Type I bend is due to the tightness of radius of curvature. The radius of curvature in the Type I bend is 38.75 ft and the radius of curvature in the Type III bend is 65.83 ft and, therefore, the Type III bend is approximately half as tight as the Type I bend. The wider radius of curvature in the Type III bend reduces the effect of spiral currents and secondary currents through the meander bend. By reducing the effect of spiral currents and secondary currents through the meander bend, the average minor loss due to meander bends through a bend is reduced, allowing HEC-RAS to estimate a more accurate average total energy loss through a meander bend.

7.3 EXAMPLE PROBLEM

The procedure presented herein may be applied to actual field projects for the purpose of calculating minor loss due to meander bends and, therefore, total energy loss through a meander bend and along a study reach. A design example is outlined in order to demonstrate how to calculate minor loss due to a meander bend using HEC-RAS output, total energy loss through a meander bend using HEC-RAS output and how to incorporate minor loss due to a meander bend in a HEC-RAS model.

7.3.1 $\bar{h}_{BEND}$ Calculation With HEC-RAS Output

Cross-sectional average minor loss due to a meander bend is calculated with the π_5 method outlined in Section 7.1.3. Using an example problem, descriptions of each step are shown below:

Step 1. Define project area

This example is an imaginary study reach along the Middle Rio Grande in New Mexico. As a result of dam placement, the study reach experienced a shift in channel morphology from a straight braided river to a meandering river. The study reach is a meandering river, 2.5 miles in length and there are ten meander bends along the study reach. The meander bends have altered geomorphic characteristics in the study reach. Geomorphic changes included bank erosion and bend migration.

Step 2. Collect appropriate data during site assessment

During the site assessment, data needed to be collected in order to build the most representative HEC-RAS model. Field data included a field survey, roughness

coefficients at all defined cross sections, and the location of significant expansions/contractions.

A field survey of the study reach included a cross-sectional survey of all relevant cross sections and a thalweg survey. Along the study reach, ninety-nine cross-sectional surveys were collected to define ten meander bends. The thalweg survey defined the bed slope through the study reach and downstream of the study reach. Bed slope through the study reach and downstream of the study reach was estimated as 0.000863 ft/ft. The downstream bed slope was used as the boundary condition in HEC-RAS.

Along with field surveying, roughness coefficients were observed for the ninety-nine defined cross sections. Roughness coefficients were identified for the left overbank, channel, and right overbank of each cross section. For the imaginary study reach, observed roughness coefficients for the left overbank and right overbank were uniformly 0.050 and the channel was uniformly 0.045.

Additional notes were needed to identify the location of significant contraction and expansion reaches. Contraction and expansion reaches, as illustrated in Figure 2.2, are defined facing downstream. During the site assessment, abrupt contraction reaches were observed along the study reach. Each abrupt contraction connected adjacent meander bends and, therefore, nine contraction reaches were noted. Abrupt contractions are indicated with a contraction coefficient of 0.6. Refer to Table 2.1 for a list of contraction and expansion coefficients.

Step 3. Build HEC-RAS model

Using field data collected in Step 2 in addition to other sources of data such as USGS stage vs. discharge records, build a HEC-RAS model representing the 2.5-mile

study reach. The HEC-RAS model includes one plan with a representative geometry data file and steady flow file of the study reach.

Cross-sectional survey data, roughness coefficients, and contraction coefficients are entered in the geometry data file. Use a planform view of the cross-sectional survey to calculate the distance between cross sections. Distances between cross sections are entered in the geometry data file. Figure 7.2 illustrates the HEC-RAS interface used to enter geometry data.

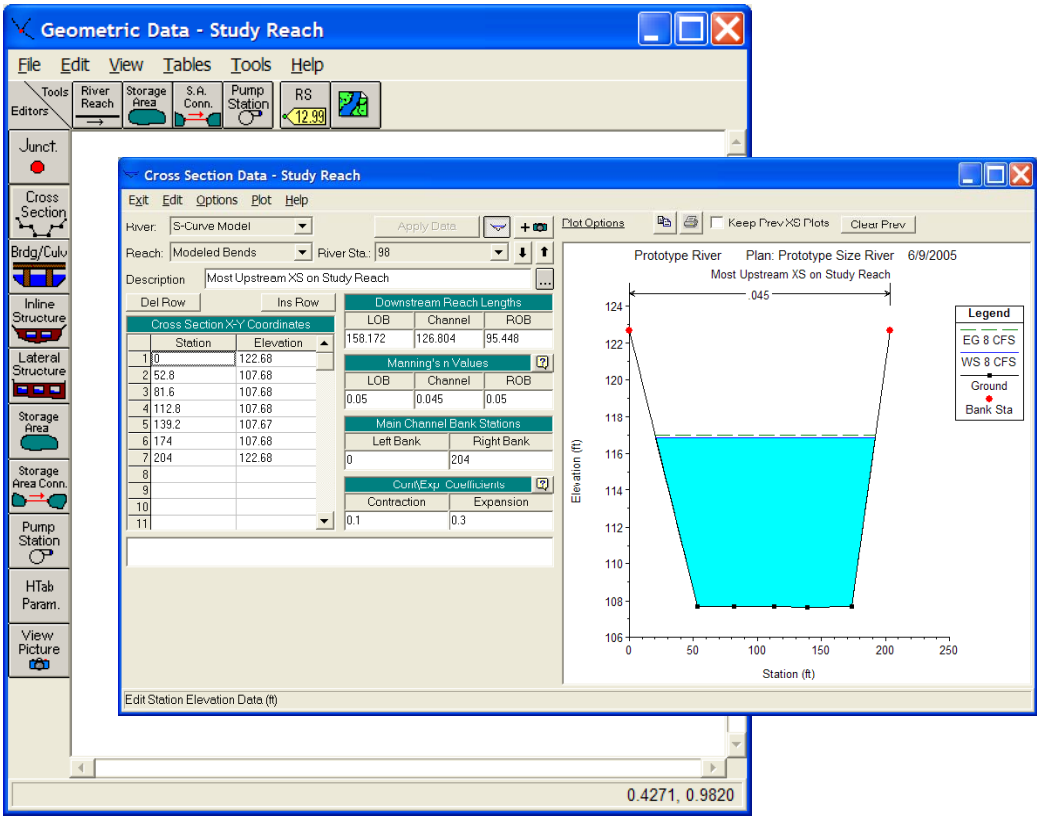

Figure 7.2. HEC-RAS Cross-section Interface

In addition to geometry information, flow data must be entered in a steady flow file in order to run the model. Steady flow data include flow rates of interest and a boundary condition. The flow rate of interest represents a flow condition present in the

study reach. For the study reach, 4,000 cfs was selected as the flow rate of interest and is defined at the most upstream cross section in HEC-RAS. Figure 7.3 presents the interface used to enter the flow rate in the HEC-RAS model. Assuming there are no tributaries, the flow rate remains constant along the 2.5-mile study reach.

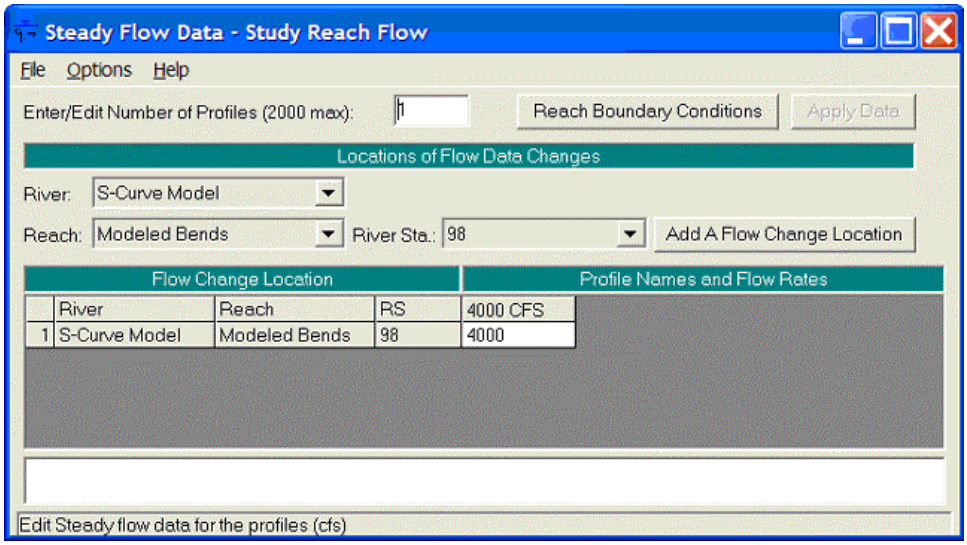

Figure 7.3. HEC-RAS Steady Flow Interface

Once the flow rate is entered in the steady flow file, a boundary condition must be specified. A downstream boundary condition is required since the flow is assumed subcritical. Using the defined HEC-RAS options, the downstream boundary condition is selected as “Normal Depth” and, therefore, the downstream bed slope is entered in HEC-RAS. Figure 7.4 shows the HEC-RAS interface used for entering the boundary condition.

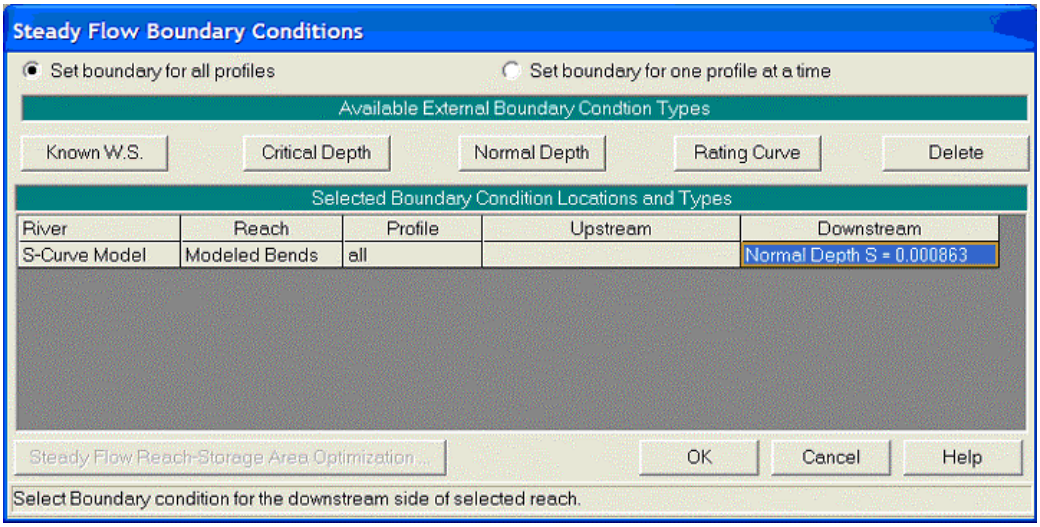

Figure 7.4. HEC-RAS Boundary Condition Interface

Step 4. Run HEC-RAS

Using the plan created in Step 3, run the HEC-RAS model. Create an output table in HEC-RAS including top width and friction loss. An example of the output table interface is shown in Figure 7.5.

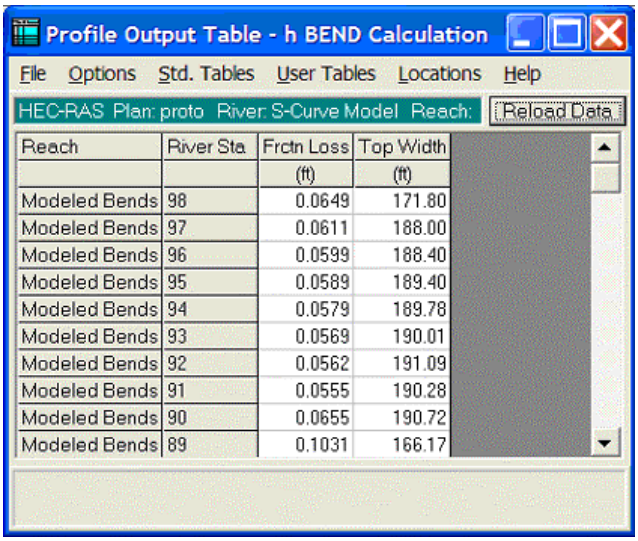

Reach	River Sta	Frctn Loss (ft)	Top Width (ft)
Modeled Bends	98	0.0649	171.80
Modeled Bends	97	0.0611	188.00
Modeled Bends	96	0.0599	188.40
Modeled Bends	95	0.0589	189.40
Modeled Bends	94	0.0579	189.78
Modeled Bends	93	0.0569	190.01
Modeled Bends	92	0.0562	191.09
Modeled Bends	91	0.0555	190.28
Modeled Bends	90	0.0655	190.72
Modeled Bends	89	0.1031	166.17

Figure 7.5. HEC-RAS Output Table Interface

Step 5. Calculate $\overline{TW}$

In order to calculate average top width, copy the top width column in the HEC-RAS output file into a Microsoft® Excel table. Use these data to estimate average top width in each meander bend. Average top width results are shown in Table 7.7.

Table 7.7. $\overline{TW}$ Results

Bend	$\overline{TW}$ (ft)
1 (U/S)	189.45
2	138.42
3	189.57
4	138.62
5	191.27
6	139.44
7	188.51
8	137.32
9	191.50
10 (D/S)	135.99

Step 6. Estimate r_c

Radius of curvature is estimated for each meander bend using aerial photographs of the study reach. For the imaginary study reach, radius of curvature estimates for each meander bend are shown in Table 7.8.

Table 7.8. r_c Measurements

Bend	r_c (ft)
1 (U/S)	465
2	790
3	465
4	790
5	465
6	790
7	465
8	790
9	465
10 (D/S)	790

Step 7. Calculate π_5

π_5 is defined in Equation 7.1. Calculate π_5 using average top width calculated in Step 5 and radius of curvature estimated in Step 6. Table 7.9 presents π_5 results.

Table 7.9. π_5 Results

Bend	$\overline{TW}$ (ft)	r_c (ft)	π_5
1 (U/S)	189.45	465	2.45
2	138.42	790	5.71
3	189.57	465	2.45
4	138.62	790	5.70
5	191.27	465	2.43
6	139.44	790	5.67
7	188.51	465	2.47
8	137.32	790	5.75
9	191.50	465	2.43
10 (D/S)	135.99	790	5.81

Step 8. Calculate $\bar{h}_{BEND}/\bar{h}_{Sf}$

Calculate $\bar{h}_{BEND}/\bar{h}_{Sf}$ using Equation 7.2, which illustrated the relationship between π_5 and $\bar{h}_{BEND}/\bar{h}_{Sf}$. π_5 was calculated in Step 7. $\bar{h}_{BEND}/\bar{h}_{Sf}$ results are presented in Table 7.10.

Table 7.10. $\bar{h}_{BEND}/\bar{h}_{Sf}$ Results

Bend	π_5	$\bar{h}_{BEND}/\bar{h}_{Sf}$
1 (U/S)	2.45	1.31
2	5.71	0.30
3	2.45	1.31
4	5.70	0.30
5	2.43	1.32
6	5.67	0.30
7	2.47	1.30
8	5.75	0.29
9	2.43	1.33
10 (D/S)	5.81	0.29

Step 9. Calculate $\bar{h}_{BEND}$

Calculate cross-sectional average minor loss due to a meander bend using Equation 7.3. In order to complete this calculation, copy the average friction loss (h_{Sf}) column in the HEC-RAS output table into a Microsoft® Excel table. Use these values to calculate cross-sectional average, average friction loss in each meander bend. Cross-sectional average, average friction loss is calculated by averaging the average friction loss estimates for an individual meander bend. Once cross-sectional average, average friction loss is calculated for each meander bend, calculate cross-sectional average minor loss due to a meander bend using Equation 7.3. Cross-sectional average minor loss due to meander bend results are shown in Table 7.11. Cross-sectional average minor loss due

to meander bend results are used to estimate the average total energy loss through a meander bend in Section 7.3.2.

Table 7.11. $\bar{h}_{BEND}$ Results

Bend	$\bar{h}_{BEND}$ (ft)
1 (U/S)	0.077
2	0.045
3	0.076
4	0.045
5	0.075
6	0.044
7	0.073
8	0.042
9	0.071
10 (D/S)	0.039

7.3.2 $\bar{h}_T$ Calculation With HEC-RAS Output

Previous analysis in Step 9 of the π_5 method provides all necessary data to compute average total energy loss through a meander bend. Average total energy loss through a meander bend is calculated with Equation 7.4 and Equation 7.5. Average total energy loss through a meander bend results are presented in Table 7.12.

Table 7.12. $\bar{h}_T$ Results

Bend	$\bar{h}_T$ (ft)
1 (U/S)	0.676
2	1.170
3	0.671
4	1.158
5	0.661
6	1.127
7	0.641
8	1.109
9	0.618
10 (D/S)	1.062
Σ	**8.894**

7.3.3 Comparison Between $\bar{h}_T$ Calculated With Modified HEC-RAS Data Set and Unmodified HEC-RAS Data Set

Analysis was completed in order to compare the average total energy loss through a meander bend using modified HEC-RAS data and unmodified HEC-RAS data. The modified HEC-RAS data set applies the π_5 method to HEC-RAS output. The unmodified HEC-RAS data set strictly uses HEC-RAS output tables to calculate total energy loss through a meander bend.

The modified HEC-RAS data set was used in Section 7.3.2 in order to estimate the average total energy loss through each meander bend and along the 2.5-mile study reach. From Table 7.12, the estimate of average total energy loss along the 2.5-mile study reach was 8.9 ft.

The unmodified HEC-RAS data set used HEC-RAS output from the same model to calculate the average total energy loss through a meander bend. Average total energy loss through a meander bend and along the 2.5-mile study reach was calculated using HEC-RAS output for friction loss. Friction loss is assumed to be equal to total energy

loss since the primary source of energy loss through a meander bend in a 1-D HEC-RAS model is friction. Table 7.13 presents the average total energy loss results through each meander bend and along the 2.5-mile study reach. The average total energy loss along the 2.5-mile study reach was 5.8 ft.

Using the two data sets, it is important to understand if the average total energy loss through a meander bend estimated with unmodified HEC-RAS output is more or less conservative than the average total energy loss estimated with modified HEC-RAS output. If the unmodified HEC-RAS data set underestimates the average total energy loss, errors can potentially occur in design projects, for instance, in bendway-weir design. The modified HEC-RAS data set calculated the average total energy loss along the 2.5-mile study reach as 8.9 ft. The unmodified HEC-RAS data set calculated the average total energy loss to be 5.8 ft along the 2.5-mile study reach, which is 35% less than the modified HEC-RAS data set. Such an alarming difference between the two estimates of average total energy loss suggests how significant minor loss due to a meander bend is in determining total energy loss. Since minor loss due to a meander bend is significant, further analysis needs to be completed to incorporate minor loss due to a meander bend in HEC-RAS iterations.

Table 7.13. $\bar{h}_T$ Results for Unmodified HEC-RAS Output

Bend	$\bar{h}_T$ (ft)
1 (U/S)	0.292
2	0.901
3	0.290
4	0.890
5	0.284
6	0.864
7	0.278
8	0.858
9	0.266
10 (D/S)	0.826
Σ	**5.750**

7.3.4 n_{EFF} Calculation

In order to incorporate minor loss due to a meander bend into HEC-RAS, a selected term was modified in the model. The term used to incorporate minor loss due to a meander bend was the roughness coefficient (n). The modified roughness coefficient was termed effective roughness coefficient (n_{EFF}). In order to calculate the effective roughness coefficient for each meander bend, the following steps were executed:

Step 1. Create a table in Microsoft® Excel

A table needed to be created in Microsoft® Excel in order to organize necessary data for the effective roughness coefficient calculation. Table 7.14 shows an example of the Microsoft® Excel table for Bend 2. Cross-sectional average total energy loss was calculated with Equation 7.4 in Section 7.3.2 and is used in Column 1 of the table. Energy grade line (EGL_{CALC}) is calculated with the following equation:

$$EGL_{CALC} = \frac{\bar{h}_t}{\Delta x} \qquad \textbf{Equation 7.6}$$

where:

Δx = distance along the centerline of the channel between cross sections (ft);

EGL_{CALC} = energy grade line (ft/ft); and

$\bar{h}_t$ = cross-sectional average total energy loss (ft).

Discharge (Q), cross-sectional area (A), hydraulic radius (R), and the roughness coefficient (n) are copied from the HEC-RAS output table into a Microsoft® Excel table. Meander bend averages for each term are calculated in the final row of the table. Friction slope ($S_{f\ MANNING}$) is calculated using a version of Manning's equation and is calculated for the final row in the table. The version of Manning's equation used in this analysis is illustrated in Equation 2.9.

Table 7.14. Table Required for n_{EFF} Calculation

Bend	XS	$\bar{h}_t$ (ft)	EGL_{CALC} (ft/ft)	Q (cfs)	A (ft^2)	R (ft)	n	$S_{f\ MANNING}$ (ft/ft)
2	87	0.195	0.00155	4000	991.82	6.98	0.0450	
	86	0.195	0.00155	4000	982.32	6.97	0.0450	
	85	0.195	0.00155	4000	971.91	6.90	0.0450	
	84	0.195	0.00155	4000	974.60	6.91	0.0450	
	83	0.195	0.00155	4000	968.06	6.88	0.0450	
	82	0.195	0.00155	4000	955.08	6.82	0.0450	
	81	0.195	0.00155	4000	959.11	6.81	0.0450	
		0.195	**0.00155**	**4000**	**971.84**	**6.90**	**0.0450**	**0.00118**

Step 2. Calculate n_{EFF}

Use a Solver routine to change the calculated meander bend average roughness coefficient until the energy grade line is equal to friction slope. The solution found from the Solver routine is the effective roughness coefficient. Table 7.15 illustrates the cells required for the Solver routine. The yellow-shaded cell is effective roughness coefficient

and is set as the "cell to change" in the Solver routine. The light green-shaded cell is selected as the "target cell" in the Solver routine. One constraint is set in the Solver routine for $EGL_{CALC} = S_{f\,MANNING}$.

Table 7.15. Selected Cells for Solver Routine

Bend	XS	$\bar{h}_T$ (ft)	EGL_{CALC} (ft/ft)	Q (cfs)	A (ft^2)	R (ft)	n	$S_{f\,MANNING}$ (ft/ft)
2	87	0.195	0.00155	4000	991.82	6.98	0.0450	
	86	0.195	0.00155	4000	982.32	6.97	0.0450	
	85	0.195	0.00155	4000	971.91	6.90	0.0450	
	84	0.195	0.00155	4000	974.60	6.91	0.0450	
	83	0.195	0.00155	4000	968.06	6.88	0.0450	
	82	0.195	0.00155	4000	955.08	6.82	0.0450	
	81	0.195	0.00155	4000	959.11	6.81	0.0450	
		0.195	**0.00155**	**4000**	**971.84**	**6.90**	**0.0515**	**0.00155**

Step 3. Check n_{EFF}

In HEC-RAS, the average conveyance method for friction slope is used in place of Manning's equation for friction slope used in Step 2 to calculate average friction slope ($\bar{S}_{f-CONV}$). Average friction slope calculated with the average conveyance method is shown in Equation 2.10. The analysis goal is to modify the roughness coefficient in order to match the average friction slope calculated through HEC-RAS to the energy grade line using the π_5 method. Since this is the analysis goal, the effective roughness coefficients calculated in Step 2 needed to be substituted into the equation for average friction slope in order to determine if the effective roughness coefficient predicts the same slope. If $EGL_{CALC} = \bar{S}_{f-CONV}$, then the effective roughness coefficient calculated during Step 2 is the final value for the meander bend. If $EGL_{CALC} \neq \bar{S}_{f-CONV}$, then proceed to Step 4.

In order to complete this portion of the analysis, a table is set up as the example in Table 7.16. Energy grade line, flow rate, flow area, and hydraulic radius are equal to values used in Table 7.15. Effective roughness coefficient is the same at each cross section in an individual meander bend and is the value computed during the Solver routine in Step 2. Average friction slope is calculated at each cross section using Equation 2.10. In the last row of the table, average the values for energy grade line and average friction slope. The average values for energy grade line and average friction slope are used in the comparison.

Table 7.16. Comparison of EGL_{CALC} and $\overline{S}_{f\text{-}CONV}$

Bend	XS	EGL_{CALC} (ft/ft)	Q (cfs)	A (ft^2)	R (ft)	n_{EFF}	$\overline{S}_{f-CONV}$ (ft/ft)
2	87	0.00155	4000	991.82	6.98	0.05151	0.00148
	86	0.00155	4000	982.32	6.97	0.05151	0.00152
	85	0.00155	4000	971.91	6.9	0.05151	0.00154
	84	0.00155	4000	974.60	6.91	0.05151	0.00155
	83	0.00155	4000	968.06	6.88	0.05151	0.00160
	82	0.00155	4000	955.08	6.82	0.05151	0.00162
	81	0.00155	4000	959.11	6.81	0.05151	
		0.00155					**0.00157**

Step 4. Modify n_{EFF}

If it was determined in Step 3 that $EGL_{CALC} \neq \overline{S}_{f-CONV}$, then Step 4 is used to modify the effective roughness coefficient. By modifying the effective roughness coefficient, the goal of $EGL_{CALC} = \overline{S}_{f-CONV}$ is achieved. Table 7.17 presents the table required to proceed with Step 4. Initially, Table 7.17 is a copy of Table 7.16 but as Table 7.17 demonstrates, the effective roughness coefficient is modified at all cross sections

until $EGL_{CALC} = \overline{S}_{f-CONV}$. When average $EGL_{CALC} = \overline{S}_{f-CONV}$, record effective roughness coefficient.

Table 7.17. Modified n_{EFF} for $EGL_{CALC} = \overline{S}_{f\text{-}CONV}$

Bend	XS	EGL_{CALC} (ft/ft)	Q (cfs)	A (ft^2)	R (ft)	n_{EFF}	$\overline{S}_{f-CONV}$ (ft/ft)
2	87	0.00155	4000	991.82	6.98	0.05145	0.00148
	86	0.00155	4000	982.32	6.97	0.05145	0.00152
	85	0.00155	4000	971.91	6.9	0.05145	0.00154
	84	0.00155	4000	974.60	6.91	0.05145	0.00155
	83	0.00155	4000	968.06	6.88	0.05145	0.00159
	82	0.00155	4000	955.08	6.82	0.05145	0.00162
	81	0.00155	4000	959.11	6.81	0.05145	
		0.00155					**0.00155**

Step 5. Organize final list of n_{EFF}

In order to continue with the analysis, a final list of all effective roughness coefficients is required. The final list for the imaginary study reach is shown in Table 7.18.

Table 7.18. n_{EFF} for Each Meander Bend

Bend	n_{EFF}
1 (U/S)	0.06820
2	0.05145
3	0.06810
4	0.05145
5	0.06836
6	0.05150
7	0.06795
8	0.05110
9	0.06840
10 (D/S)	0.05016

7.3.5 Implementation of n_{EFF} in HEC-RAS

Once the effective roughness coefficient is calculated for each meander bend, the value must be used in the HEC-RAS analysis. Effective roughness coefficient replaces the observed roughness coefficient at all cross sections in a meander bend. For instance, Bend 1 is represented by river stations 92 to 97 and, therefore, the effective roughness coefficient of 0.0682 replaces the observed roughness coefficient of 0.045 at river stations 92 to 97. This process is completed for the entire study reach.

7.3.6 n_{EFF} Significance

Significance of the effective roughness coefficient is observed along the study reach once HEC-RAS iteratively calculated the water-surface profile and energy grade line using the effective roughness coefficient. Table 7.19 presents the results from implementing an effective roughness coefficient in HEC-RAS. Table 7.19 shows that the effective roughness coefficient increases the average total energy loss through the study reach to 6.9 ft, which is an increase of 1.1 ft. The purpose of implementing the effective roughness coefficient in HEC-RAS was to increase friction loss from 5.8 ft to 8.9 ft, which is a difference of 3.1 ft. The HEC-RAS output of friction loss was 65% less than the desired output for friction loss using the π_5 method.

In order to understand why HEC-RAS output of average total energy loss through the study reach was 65% less than the desired output for average total energy loss through the study reach using the π_5 method, further analysis was completed. Patterns were observed between meander bends to note changes in flow depth, flow area, conveyance, and friction loss for the HEC-RAS output considering the effective

roughness coefficient and the π_5 method. From this analysis, it was observed that the π_5 method calculated average total energy loss for each meander bend independent of the other bends while HEC-RAS calculated average total energy loss given a series of meander bends. When average total energy loss was calculated for an individual bend, the average total energy loss estimate was greater than the average total energy loss calculated for a series of meander bends. Hydraulic calculations of meander bends in a series, such as in HEC-RAS, influence the calculation of the upstream bend. For instance, flow depth from the downstream bend influences the flow depth in the upstream bend through backwater calculations. Therefore, the average total energy loss calculated from meander bends in a series does not necessarily increase with the same magnitude as average total energy loss calculated from individual meander bends in the π_5 method. Comparing Table 7.13 and Table 7.19, in some cases, average total energy loss decreases once the effective roughness coefficient is implemented in HEC-RAS. Further analysis needs to be completed in order to fully understand the influence of meander bends in series on average total energy loss calculations along the study reach.

Table 7.19. $\bar{h}_T$ for HEC-RAS Output With n_{EFF}

Bend	$\bar{h}_T$ (ft)
1 (U/S)	0.477
2	0.845
3	0.474
4	0.852
5	0.479
6	0.855
7	0.485
8	0.893
9	0.543
10 (D/S)	0.962
Σ	**6.864**